lajss.org© Latin American Journal of Solids and Structures

www.lajss.org

Numerical analysis of the bandgap-inducing properties of sandwich foundations

Leonardo Antoniazzi Marques https://orcid.org/0009-0003-9750-5485, Luís Filipe do Vale Lima https://orcid.org/0000-0001-7682-2789, Euclides Mesquita https://orcid.org/0000-0001-6512-7596, Josué Labaki* https://orcid.org/0000-0003-2024-4793

School of Mechanical Engineering, University of Campinas, 200 Mendeleyev St., Campinas, 13083-860, SP, Brazil. Emails: l201083@dac.unicamp.br, l162588@dac.unicamp.br, euclides@fem.unicamp.br, labaki@unicamp.br

* Corresponding author

Abstract

This paper investigates the vibration attenuation performance of periodic foundations for surface structures. A numerical method is proposed, which considers one- or two-dimensional linear-elastic bodies under time-harmonic external load and seismic excitation. These bodies are modeled via the Finite Elements Method, while their supporting soil is modeled as a homogeneous half-space via the Indirect Boundary Element Method. Coupling between the methods is obtained by imposing direct continuity and equilibrium conditions at the interface. Three different configurations of foundations are studied: 1) no foundation, 2) homogeneous foundation, and 3) sandwich foundation – two materials layered in an alternate fashion. Material properties and thickness of the layers are selected to induce prescribed bandgaps in the response of the structure. The results are presented in terms of data that can be directly applied in engineering practice.

Keywords

Metamaterials, Vibration Attenuation, Soil-Structure Interaction, Coupled methods

Graphical Abstract

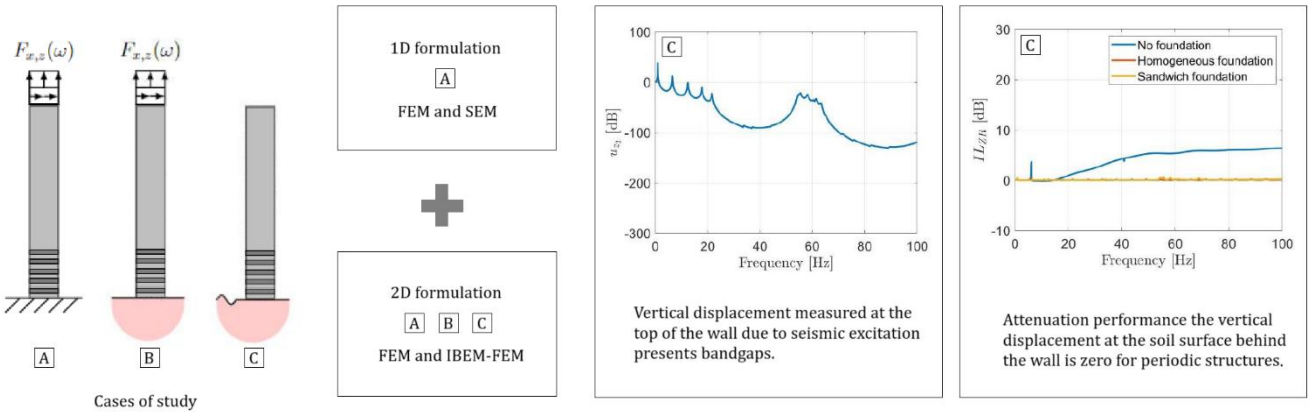

1 INTRODUCTION

In engineering applications, uncontrolled excessive vibration is something to be avoided as it can lead to structural fatigue, noise, and catastrophic failure. For vibration-sensitive structures, effective mechanisms to control excessive vibration levels are crucial. A popular method for mitigating vibration involves utilizing periodic foundations, which exploit the principles of wave propagation in periodic media to manage vibrations across a range of structures, including buildings, bridges, machinery, and electronic devices (Shi, Cheng and Xiang, 2014). Effective vibration isolation of structures can be achieved by carefully designing the periodicity profile and material properties of these foundations, which work by inducing bandgaps in the frequency response of the structure.

The application of periodic foundations for structural vibration isolation has been intensively studied in recent years. Several studies have been carried out to validate the feasibility and efficiency of this isolation system. Xiang et al. (2012) proposed a new layered periodic foundation and showed that it can induce frequency bandgaps that effectively reduce vibrations in buildings, acting as a vibration isolator. Xiong et al. (2012) studied how periodic foundations can significantly reduce the dynamic response of structures under both vertical and longitudinal ground motion, offering a new view in civil engineering applications. Pu and Shi (2018) showed that a damped layered periodic foundation with more than one unit cell significantly improved the seismic performance of the structure under ground motion in different site conditions. However, the most significant, recent papers in the area of the present study were published by Jain et al. (2021) and Elshazly and Seylabi (2023), who studied the effectiveness of sandwiched layers of concrete and rubber in inducing bandgaps in the response of structures interacting with the soil and found that these foundations can be tuned to induce bandgaps at specific frequencies of excitation.

The present paper reports on a study on the vibration attenuation performance of surface walls supported by sandwich foundations. In this paper, the term sandwich foundation is used to refer to a base interposed between the wall and its support, in which the base is made up of alternating layers of two different materials. A coupled method is used to describe the wall—soil system, which is modeled as a 2D, plane strain problem. Excitation is applied directly on the wall or impinges on the wall from seismic sources. The objective of the paper is to understand the effect of the sandwich foundation in the ground vibration attenuation performance of the wall. The paper shows selected numerical results on the attenuation performance of walls and foundations with different geometric and constitutive parameters.

2 PROBLEM STATEMENT

The problem consists of linear-elastic walls that are modeled as either one-dimensional or two-dimensional bodies of infinite length, height *H*, and width *L* (in the two-dimensional case). A portion *h* of the height of the wall, referred to in this paper as "foundation," can be made of one single material, or of alternating layers of two different materials. The different configurations for the wall and its foundation considered in this paper are (Fig. 1): (i) a homogeneous wall without a foundation, (ii) a homogeneous wall supported by a homogeneous foundation, that is, built with only one material, and (iii) homogeneous wall supported by a sandwich foundation, built with alternating layers of two different materials.

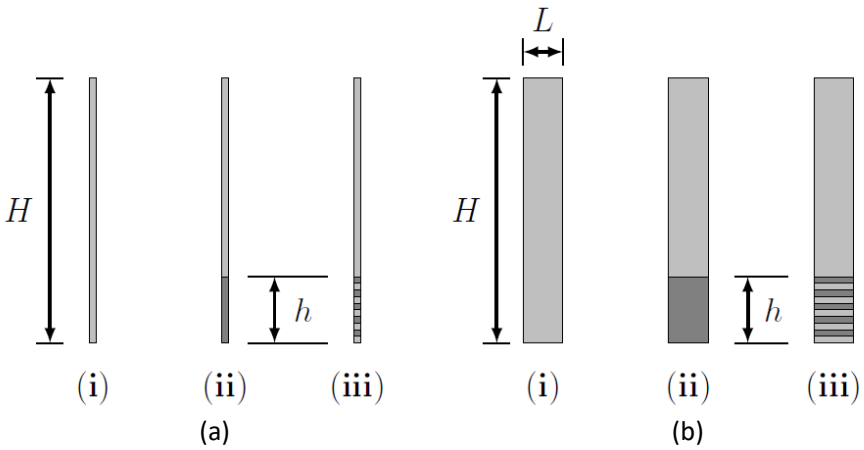

Figure 1: Configurations for (a) one- and (b) two-dimensional cases, in which light-gray and dark-gray represent different materials.

The sandwich foundation is composed of *n* identical unit cells stacked on top of each other (Fig. 2). Each unit cell is divided into two halves, each made of one out of two different materials, resulting in a foundation consisting of *2n* alternating layers of these materials.

These structures are analyzed under three distinct support scenarios (Fig. 3). In Case A, the wall is supported by a rigid base and loaded from the top with a time-harmonic vertical (*z*-direction) loading with unit magnitude. In Case B, the wall is loaded from the top and rests on a flexible soil. In Case C, the wall is subjected to excitation in the form of a time-harmonic plane Rayleigh wave of unit magnitude propagating through the soil and impinging onto the wall—soil system from its left side. The objective is to determine which configuration promotes the greatest reduction in the wall's vibration amplitude.

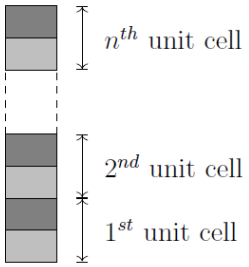

Figure 2: Unit cells of the sandwich foundation.

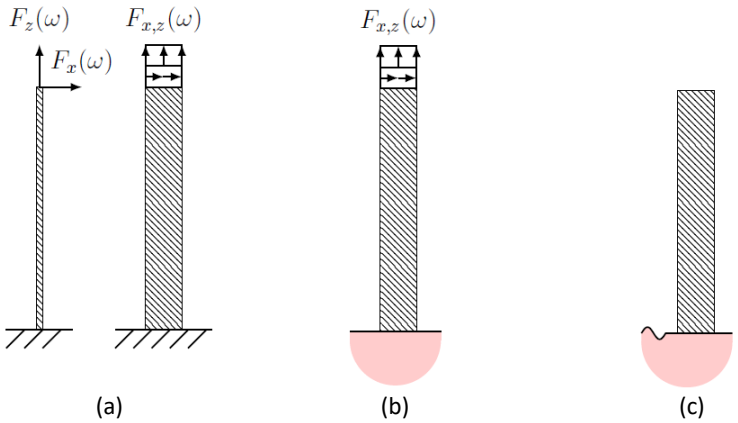

Figure 3: (a) case A, (b) case B, and (c) case C considered in the analysis.

3 FORMULATION

The main goal of this analysis is to understand the behavior of two-dimensional walls, in view of its potential for direct application in engineering practice. However, in order to provide a deeper understanding of the effect of sandwich foundation in the response of the wall, a one-dimensional model for this system is also considered. This 1D model enables one to isolate the effect of lateral energy dissipation that occurs in the 2D problem due to the Poisson effect. Both 1D and 2D models of the wall are formulated according to the classical Finite Element Method (FEM), in view of the finite dimensions of the wall and its linear-elastic behavior. For Case C, in which wall—soil interaction is considered, an Indirect Boundary Element Method (IBEM) formulation is used for the soil, so that radiation conditions and wave propagation features of the soil can be represented accurately. Additionally, a Spectral Element Method (SEM) formulation is used for the 1D wall, so that the behavior the wall as an infinitely periodic body can be first understood. This information can then be used to assess the minimum number *n* of unit cells that are necessary for the foundation of the 1D wall to behave as a bandgap-inducing metamaterial.

3.1 SEM model

The Spectral Element Method model of the one-dimensional wall problem is obtained after deriving the equation of motion for a spectral element, expressed as $\mathbf{D}_\mathrm{b}\mathbf{q} = \mathbf{F}$, in which $\mathbf{D}_\mathrm{b}$ is the dynamic stiffness matrices of one-dimensional bar elements, $\mathbf{q}$ is the vector of nodal displacements and $\mathbf{F}$ is the vector of nodal forces. Doyle (1997) provides the dynamic stiffness matrix for bar elements at a given frequency ω as

$$\boldsymbol{D}_b = \frac{ikEA}{1-e^{-i2kL}}\begin{bmatrix} 1+e^{-i2kL} & -2e^{-ikL} \\ -2e^{-ikL} & 1+e^{-i2kL} \end{bmatrix}, \tag{1}$$

in which *E*, *A* and *L* represent the Young's modulus, cross-sectional area, and length of the element, respectively, $k = \omega\sqrt{\rho/E}$, in which ρ is the mass density, and $\mathrm{i} = \sqrt{-1}$. For a periodic structure, defined as the infinite repetition of its constituent cells, the Bloch-Floquet condition is enforced (Bloch, 1929; Floquet, 1883), which can be expressed as

$$\{\mathrm{q}_r \quad -\mathrm{F}_r\}^{\mathrm{T}} = \mathrm{e}^{-\mathrm{i}k_x h_{uc}}\{\mathrm{q}_l \quad \mathrm{F}_l\}^{\mathrm{T}}, \tag{2}$$

where k_x is the wavenumber, and q_j and F_j are the displacements and forces vectors at the *j*-side of the unit cell, with *l* and *r* denoting the left and right sides of the cell, respectively. Rearranging the dynamic stiffness matrix into the transfer matrix form as presented by Nobrega et al. (2016), and substituting the resulting expression, leads to the following eigenvalue problem, which allows the computation of the wavenumbers for the periodic one-dimensional wall:

$$\mathbf{T} = \begin{bmatrix} -\mathbf{D}_{lr}^{-1}\mathbf{D}_{ll} & -\mathbf{D}_{lr}^{-1} \\ \mathbf{D}_{rl} - \mathbf{D}_{rr}\mathbf{D}_{lr}^{-1}\mathbf{D}_{ll} & -\mathbf{D}_{rr}\mathbf{D}_{lr}^{-1} \end{bmatrix}, \quad \mathbf{D}_{\mathrm{b}} = \begin{bmatrix} \mathbf{D}_{ll} & \mathbf{D}_{lr} \\ \mathbf{D}_{rl} & \mathbf{D}_{rr} \end{bmatrix}, \tag{3}$$

$$\mathbf{T}\{\mathbf{q}_l \quad \mathbf{F}_l\}^{\mathrm{T}} = \mathrm{e}^{-\mathrm{i}k_x h_{uc}}\{\mathbf{q}_l \quad \mathbf{F}_l\}^{\mathrm{T}}. \tag{4}$$

3.2 FEM model

For the one-dimensional FEM model of the wall under vertical loads, the wall is described as an assembly of two-noded, one-dimensional finite bar elements with one displacement degree of freedom per node, the stiffness and mass matrices of which are given by (Rao, 2011)

$$\mathbf{K}_{\mathrm{bar}} = \frac{EA}{h_e}\begin{bmatrix} 1 & -1 \\ -1 & 1 \end{bmatrix}, \quad \mathbf{M}_{\mathrm{bar}} = \frac{\rho A h_e}{6}\begin{bmatrix} 2 & 1 \\ 1 & 2 \end{bmatrix}, \tag{5}$$

in which, h_e is the length of the element.

In the 2D case, the wall is discretized using four-noded, isoparametric, linear-elastic quadrilateral finite elements, each having two degrees of freedom per node. Elemental stiffness and mass matrices $\mathbf{K}_e$ and $\mathbf{M}_e$ are given by (Bathe, 2006)

$$\mathbf{K}_e = \int_{-1}^{1}\int_{-1}^{1} \mathbf{B}^{\mathrm{T}}\,\mathbf{C}\mathbf{B}|\mathbf{J}|d\xi d\eta, \quad \mathbf{M}_e = \rho\int_{-1}^{1}\int_{-1}^{1} \mathbf{N}^{\mathrm{T}}\,\mathbf{N}|\mathbf{J}|d\xi d\eta, \tag{6}$$

in which ξ and η are natural coordinates describing the space in which the finite elements are formulated, **B** is the strain matrix, **C** is the constitutive matrix, **J** is the Jacobian operator transforming between the natural (ε, η) space and the physical (x,z) space, and **N** is the matrix of shape functions. The dynamic stiffness matrix for the wall is assembled from $\mathbf{K}_e$ and $\mathbf{M}_e$ according to $\bar{\mathbf{K}} = \mathbf{K}_{\mathrm{g}} - \omega^2\mathbf{M}_{\mathrm{g}}$, in which $\mathbf{K}_g$ and $\mathbf{M}_g$ are global stiffness and mass matrices, respectively, and ω is the frequency of excitation. The equation of motion for the wall is given by $\bar{\mathbf{K}}\mathbf{u} = \mathbf{f}$, in which **u** and **f** are the nodal displacement and force vectors, respectively.

3.3 IBEM-FEM coupling

In the 2D wall—soil contact problem, the soil is modeled as a two-dimensional, isotropic, homogeneous half-space, the response of which is obtained via the discretization of its free surface in terms of constant boundary elements. Rajapakse et al. (1991) derived solutions for the boundary elements describing this medium, which are given by

$$u_{xx} = -\frac{2}{\pi c_{44}\delta}\int_0^\infty \frac{1}{R}\left(\eta_3\bar{\omega}_1\mathrm{e}^{\delta\xi_1 z} - \eta_4\bar{\omega}_2\mathrm{e}^{\delta\xi_2 z}\right)\cos(\delta\zeta x)\,\mathrm{d}\zeta, \tag{7a}$$

$$u_{zx} = -\frac{2\mathrm{i}}{\pi c_{44}\delta}\int_0^\infty \frac{1}{R}\left(\eta_3\bar{\omega}_1\mathrm{e}^{\delta\xi_1 z} - \eta_4\bar{\omega}_2\mathrm{e}^{\delta\xi_2 z}\right)\sin(\delta\zeta x)\,\mathrm{d}\zeta, \tag{7b}$$

$$u_{xz} = \frac{2\mathrm{i}}{\pi c_{44}\delta}\int_0^\infty \frac{1}{R}\left(\eta_2\bar{\omega}_1\mathrm{e}^{\delta\xi_1 z} - \eta_1\bar{\omega}_2\mathrm{e}^{\delta\xi_2 z}\right)\sin(\delta\zeta x)\,\mathrm{d}\zeta, \text{ and} \tag{7c}$$

$$u_{zz} = \frac{2}{\pi c_{44}\delta}\int_0^\infty \frac{1}{R}\left(\eta_2\bar{\omega}_1\mathrm{e}^{\delta\xi_1 z} - \eta_1\bar{\omega}_2\mathrm{e}^{\delta\xi_2 z}\right)\cos(\delta\zeta x)\,\mathrm{d}\zeta, \tag{7d}$$

in which u_{ij} denotes displacement in the *i*-direction due to loads in the *j*-direction, in which $\zeta = \lambda/\delta$, $\alpha = c_{33}/c_{44}$, $\beta = c_{11}/c_{44}$, $\kappa = 1 + c_{13}/c_{44}$, $\delta^2 = \rho\omega^2/c_{44}$, $R = \frac{\eta_1\eta_3 - \eta_2\eta_4}{\sin(\delta\zeta\alpha)}\zeta$, $\xi_{1,2}^2 = \left(\gamma\zeta^2 - 1 - \alpha \pm \sqrt{\Phi}\right)/(2\alpha)$, $\Phi = (\gamma\zeta^2 - 1 - \alpha)^2 - 4\alpha[\beta\zeta^4 - (1+\beta)\zeta^2 + 1]$, $\gamma = 1 + \alpha\beta - \kappa^2$, $\bar{\omega}_{1,2} = \left(\alpha\xi_{1,2}^2 - \zeta^2 + 1\right)/(-i\kappa\zeta\xi_{1,2})$, $\eta_{1,2} = -\xi_{1,2}\bar{\omega}_{1,2} + i\zeta$, $\eta_{3,4} = (\kappa - 1)i\zeta\bar{\omega}_{2,1} - \alpha\xi_{2,1}$, and $c_{11} = c_{33} = \frac{E(1-\nu)}{(1+\nu)(1-2\nu)}$, $c_{12} = c_{13} = \frac{E\nu}{(1+\nu)(1-2\nu)}$, $c_{44} = \frac{E}{2(1+\nu)}$, in which E is the Young's modulus, ν is the Poisson ratio, and ρ is the mass density.

The coupling between the soil and the wall can be represented by the inclusion of interface forces $\mathbf{f}_s$, which arise at the bottom of the wall due to the presence of the soil. The modified equation of motion for the nodes at the interface can be expressed as $\bar{\mathbf{K}}'\mathbf{u}' = \mathbf{f}' - \mathbf{f}_s$, in which $\bar{\mathbf{K}}'$, $\mathbf{u}'$ and $\mathbf{f}'$ are, respectively, the dynamic stiffness matrix, and vectors of nodal displacement and forces of the interface nodes. The distribution of contact forces $\mathbf{f}_s$ experienced by the nodes of the structure must be in equilibrium with the contact tractions experienced by the soil at the interface. This distribution is unknown, and can be approximated by piece-wise constant fictitious contact tractions $\mathbf{t}_s$, which are also unknown. The equilibrium condition between $\mathbf{f}_s$ and $\mathbf{t}_s$ can be stated as $\mathbf{f}_s = \mathbf{A}\mathbf{t}_s$, in which **A** is a purely geometric transformation matrix. The equation of motion for the nodes at the wall—soil interface can be rewritten as

$$\bar{\mathbf{K}}'\mathbf{u}' + \mathbf{A}\mathbf{t}_s = \mathbf{f}'. \tag{8}$$

For the case in which the wall—soil system is subjected to Rayleigh wave excitation, the excitation is described in Equation 8 in terms of nodal displacements at the wall—soil interface **u'**. In this case, the presence of the wall on the soil surface causes incident seismic waves $\mathbf{s}^{(i)}$ to be partially scattered into a scatter component $\mathbf{s}^{(s)}$, so that the resulting displacement $\mathbf{w}_s$ at the interface is the sum of these two parts (Fairweather et al., 2003):

$$\mathbf{w}_s = \mathbf{s}^{(i)} + \mathbf{s}^{(s)}. \tag{9}$$

The scattered portion can be expressed in terms of the contact tractions $\mathbf{t}_s$ as

$$\mathbf{s}^{(s)} = \mathbf{U}\mathbf{t}_s, \tag{10}$$

in which **U** is the influence matrix of the soil, the terms of which are described in Equation 7. Displacements $\mathbf{w}_s$ can also be expressed in terms of the structural displacement $\mathbf{u}'$ at the interface as

$$\mathbf{w}_s = \mathbf{D}\mathbf{u}', \tag{11}$$

in which **D** is a purely geometric transformation matrix. Substituting Equations 11 and 10 into Equation 9 yields

$$\mathbf{D}\mathbf{u}' - \mathbf{U}\mathbf{t}_s = \mathbf{s}^{(i)}. \tag{12}$$

The reader is referred to Carneiro et al. (2022) for a full expression of matrices **A** and **D**. The continuity condition expressed by Equation 12 assumes perfectly bonded contact between the wall and the soil, which is a reasonable consideration for this problem. Expanding this equation of motion of the wall—soil interface to all nodes of the wall results in the equation of motion for the wall—soil system:

$$\begin{bmatrix} \bar{\mathbf{K}} & \begin{bmatrix}\mathbf{0}\\ \mathbf{A}\end{bmatrix} \\ \begin{bmatrix}\mathbf{D} & \mathbf{0}\end{bmatrix} & -\mathbf{U} \end{bmatrix} \begin{Bmatrix} \mathbf{u} \\ \mathbf{t}_s \end{Bmatrix} = \begin{Bmatrix} \mathbf{0} \\ \mathbf{s}^{(i)} \end{Bmatrix}. \tag{13}$$

4 NUMERICAL RESULTS

This section presents and discusses results obtained with the numerical models described in the previous sections. For the sake of these discussions, the origin of the *x—z* coordinate system is placed so that *z=0* corresponds to the free surface of the soil, and *x=0* is aligned with the center line of the wall. The results in this section are presented in terms of the vertical displacements $u_z(\omega)$ at different points of the body of the wall. The quantity $u_{z1}(\omega)$ denotes the displacement of the upper side of the first unit cell, at the bottom of the wall (at a vertical distance $z = h/(2n)$ from the base, in which n=5 is the number of unit cells used in the sandwich foundation). This point is selected as a representative point in Case A (Figure 3a) because, in this case, the displacements at *z=0* are zero, due to the rigid base on which the wall is installed.

Table 1 list the properties of the materials used in the analysis. These values were chosen because of their applicability in engineering practice. All results consider walls with height H=4m, width L=1m, and foundations with h=1m when applicable.

Table 1 Material properties.

Material	c_s [m/s]	c_p [m/s]	ρ [kg/m³]	E [MPa]	ν[1] [-]
Concrete	-	-	2,400	3.00E10	0.2
Rubber[2]	-	-	1,300	1.37E5	0.2[1]
Soil	250	1,470	1,945	-	-

[1] Some results consider varying values for ν for the rubber material.

4.1 Case A: rigid base

Figure 4 shows the frequency response of the 1D models considered in Case A. All results in this section are computed at z=h/(2n). The curve marked with an "SEM" label indicates the response of the infinitely periodic 1D body obtained via the SEM method, while the curve marked with the "FEM" label indicates the response of the 1D walls with sandwich foundations. A convergence analysis was performed for various numbers of unit cells, indicating that *n=5* unit cells is sufficient to represent the period behavior exhibited by the infinitely periodic model. Figure 4b shows the dispersion diagram obtained with the SEM model, with gray bands indicating the frequency bands in which energy is barred from propagating in the structure, due to the periodicity of the cells. These gray bands were reproduced in Figure 4a as well, illustrating the effect of the bandgaps in the vibration magnitude of both models. The discrepancy between the two curves comes from the fact that the FEM model is not infinitely periodic, but rather a finite body with a sandwich foundation that exhibits nearly period behavior. The main conclusion from these results is that a relatively small finite number of cells in the sandwich foundation is sufficient to impart bandgap-inducing properties to the system.

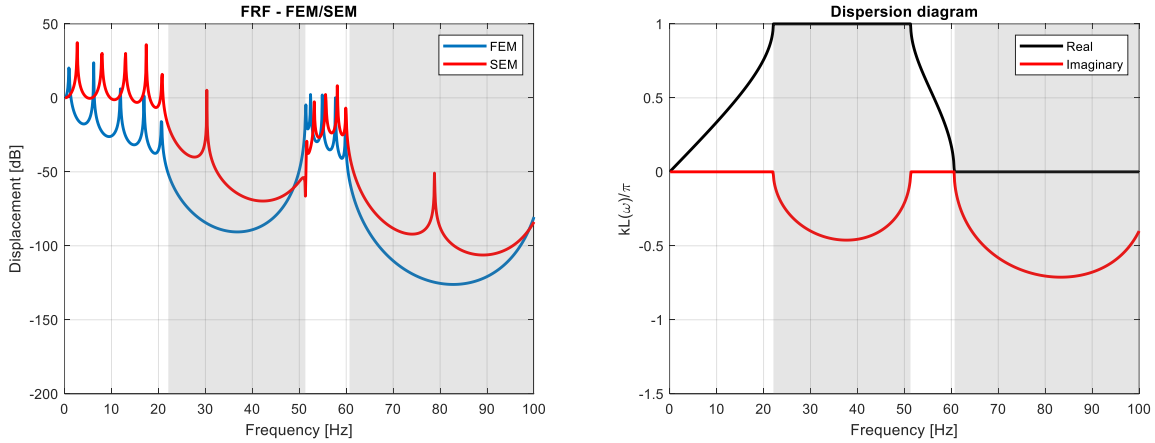

(a) (b)

Figure 4: (a) Displacement of the 1D wall and (b) dispersion diagram for the 1D wall in configuration (iii) considering a concrete wall with a concrete-rubber sandwich foundation.

Figure 5 shows a comparison between the response of the 1D wall supported by a rigid base (Case A) in all three configurations (i), (ii) and (iii) (Figure 1b). The inclusion of a homogeneous foundation has a significant effect in the response of the system, but bandgaps in the frequency response of the wall are only observed when the sandwich foundation is introduced.

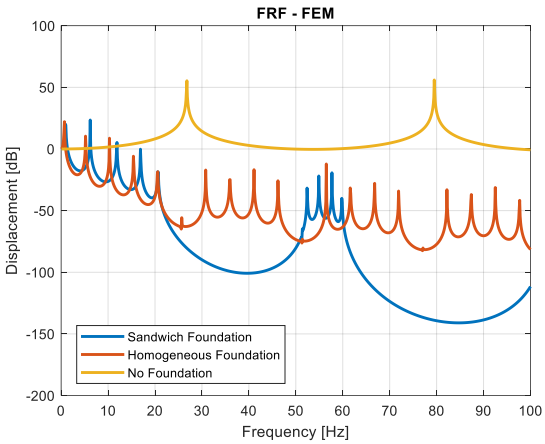

Figure 5: Response of 1D walls considering concrete wall with a concrete-rubber sandwich foundation.

The main difference between the one- and two-dimensional model of this problem is the ability of the latter to undergo transverse deformation when subjected to the vertical loading, because of the Poisson effect. Figure 6 shows results for the 2D wall when various values of Poisson ratio are considered for the rubber material used in the sandwich foundation. In this analysis, the Poisson's ratio of the concrete is fixed at $\nu = 0.2$, while the Poisson's ratio of rubber varies from $\nu = 0$ to $\nu = 0.4$. These results show that the Poisson's ratio of the rubber layers directly influences the response of the wall. These results show that larger values of ν hinder the ability of the sandwich foundation to induce bandgaps, which is connected to the transverse energy dissipation resulting from the greater Poisson effect in this case. When ν=0, no energy dissipation in the transverse direction is present, and the sandwich foundation can induce bandgaps in the vertical response of the wall.

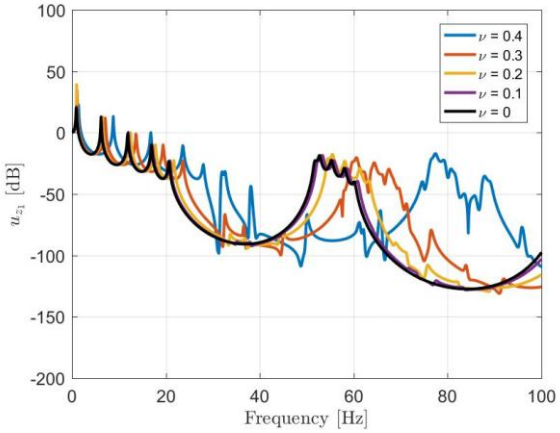

Figure 6: Poisson's ratio effect for the 2D concrete wall with a concrete-rubber sandwich foundation.

4.2 Case B: flexible soil

Figure 7 shows the frequency responses for the 2D models considered in Case B, in which the wall is supported by a flexible soil (Fig. 3b). These results are computed at z=0 for cases (i), (ii) and (iii) shown in Fig. 1b. Figure 7a shows that the presence of the soil has a significant damping effect in the response of the system in cases (i) and (ii), in which the sandwich foundation is not present. This can be seen comparing the "No foundation" case (i) from Fig. 7a with that from Fig. 5. This is due to the geometric damping properties of the soil as an unbounded, energy-dissipating medium.

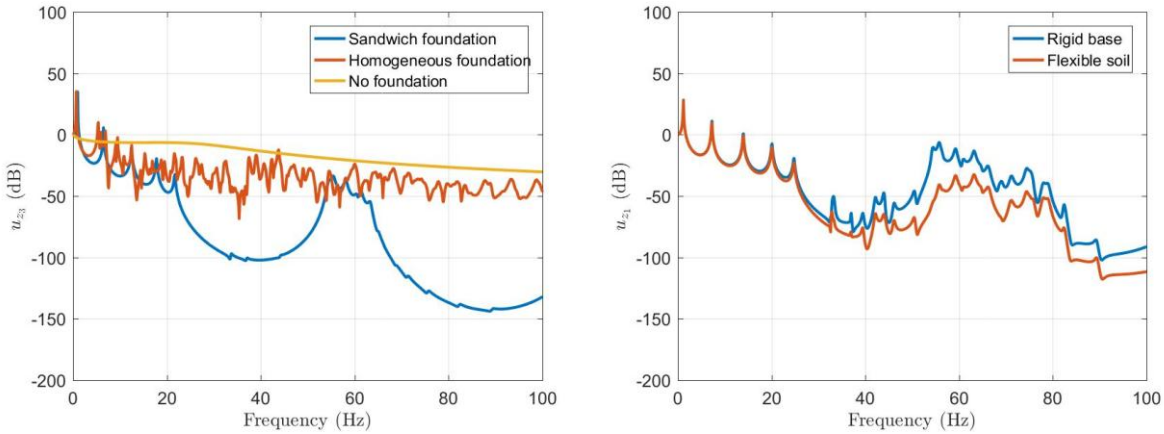

Figure 7: vertical responses at $z = 0$ for 2D walls considering concrete wall and concrete-rubber foundation.

Figure 7b, however, shows that the inclusion of the flexible soil has a negligible effect in the response of the system when a sandwich foundation is considered. This figure compares the cases in which the wall with sandwich foundation is supported by a rigid base with that in which the wall is supported by the soil. This is understandable, since the vibration originating from the top of the wall in this Case B (Fig. 3b) is mostly filtered out by the sandwich foundation before it reaches the soil, rendering ineffective the geometric damping properties of the soil.

4.3 Case C: seismic excitation

Figure 8 shows the frequency responses of 2D walls supported by the soil, in the case in which the system is under Rayleigh wave excitation. Figures 8a and 8b show respectively the vibration measured at the bottom and at the top of the wall. In this case, vibration propagates from the bottom to the top of the wall, crossing through the homogeneous or periodic foundation. Figure 8 shows that vibration attenuation occurs at the top of the wall, after the vibratory energy passes through the foundation. Together with the results from Fig. 7b, this supports the idea that the foundation, especially the periodic foundation, works as a filter, isolating the structure from its surroundings, regardless of each side of this filter vibratory energy is applied. Figure 8a shows that the inclusion of the foundation causes the wall to behave as if the wall did not exist, from the point of view of its effect on the propagation of the Rayleigh wave. This hinders even the positive ground vibration attenuation effects that homogeneous walls have been found to provide (Carneiro et al., 2022).

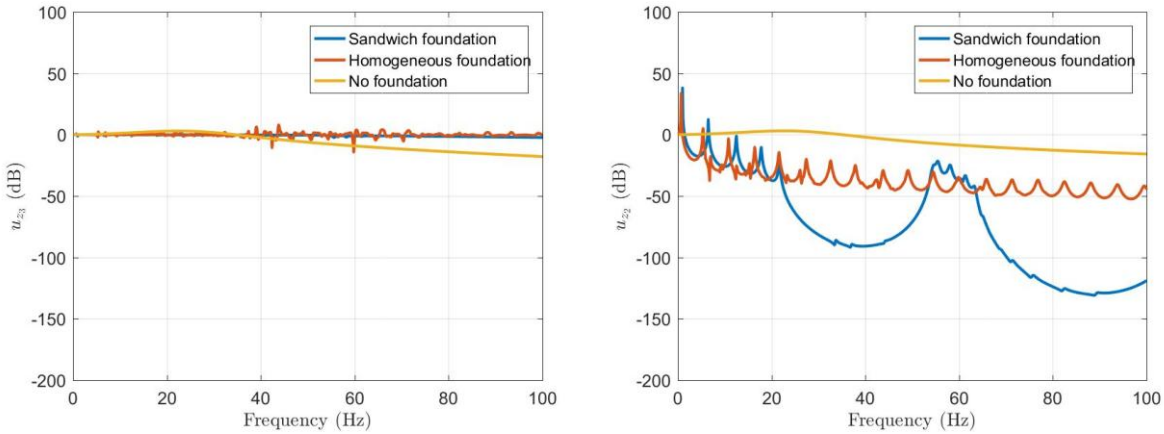

Figure 8: Vertical response at (a) $z = 0$ and (b) $z = H$ for 2D walls in configuration (iii) considering a concrete wall with concrete-rubber foundation.

Finally, we assessed the ability of the wall to reduce vibration of a point behind it, i.e., x>0. This is important for engineering practice, because the wall could be used to protect sensitive target structures by being installed between the source of vibration and the target structure. In this paper, this performance is evaluated by measuring the vibration

magnitude in the z-direction at a point P located 20 m behind the wall ($x = 20$ m, $z = 0$). Results at the point where the wall is installed ($x = 0, z = 0$) are included for comparison. The vibration attenuation performance of the wall is measured according to the insertion loss, defined as

$$IL_{zR} = 20\log_{10}\left|\frac{u_{zR}^{(b)}(\omega)}{u_{zR}^{(a)}(\omega)}\right|, \tag{26}$$

in which $u_{zR}^{(b)}(\omega)$ and $u_{zR}^{(a)}(\omega)$ indicate the displacement of P in z-direction without and with the presence of the wall in the system, respectively. Positive values of insertion loss indicate that the wall induces attenuation of the ground vibration, while negative values indicate that the wall leads to vibration amplification.

Figure 9 shows the insertion loss provided by 2D concrete walls in the three configurations listed in Fig. 1. The results indicate that walls with homogeneous and sandwich foundations have a negligible effect on the vibration propagated through the soil, both at the installation point and at point P. In contrast, walls without foundations produce significant attenuation of the vibration, reaching up to 35 dB (Figure 18a), which is consistent with Carneiro et al. (2022). Once again, this indicates that the sandwich foundation acts as a filter for the vibration coming from the soil, thereby cancelling the attenuation mechanisms of the wall as a local resonator.

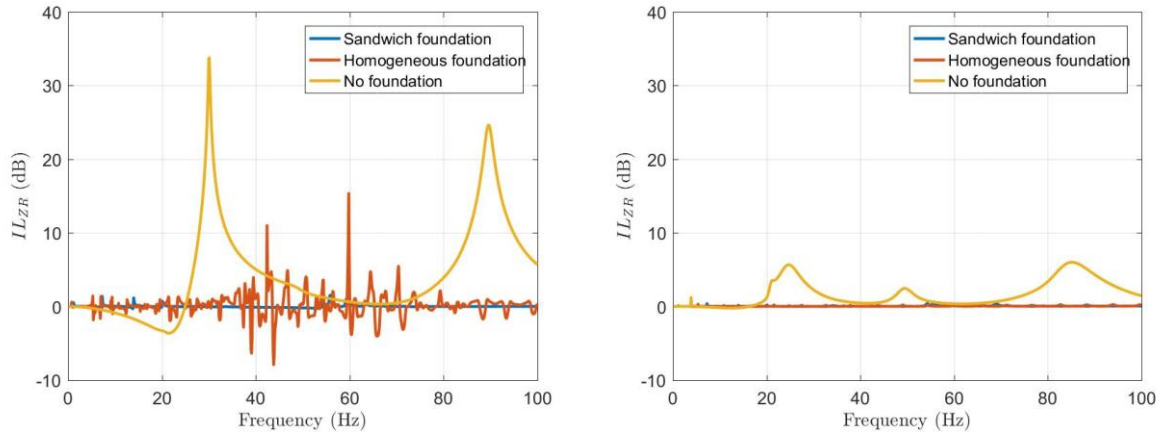

Figure 9: Vertical insertion loss at (a) $x = 0$ and (b) $x = 20$ measured at the soil surface for 2D walls considering concrete wall with concrete-rubber foundation.

4 CONCLUSIONS

This paper presented a study on the ground vibration attenuation performance of surface walls supported by sandwich foundations. The analysis considered homogeneous walls without foundation, as well as walls with homogeneous and sandwich foundations, supported either by a rigid base or by flexible soil. The results indicated that an SEM analysis of 1D models can accurately predict the frequency bands where significant attenuation occurs in the responses of 2D structures, provided that the Poisson's ratio of the materials of the 2D structures is sufficiently small. More importantly, sandwich foundations were found to act as a filter, isolating the dynamic response of the wall from that of the soil. This effect is beneficial for soil vibration when the excitation originates from the structure, but it hinders the attenuation of soil vibration when the excitation comes from the soil, as it prevents the wall from functioning as an effective vibration attenuator.

ACKNOWLEDGMENTS

The research leading to this article has been funded by the São Paulo Research Foundation (Fapesp) through grants 2013/08293-7 (CEPID) and 2022/02753-5 and by the National Council for Scientific and Technological Development (CNPq) through grant 420314/2023-7. The support of Capes and Faepex/Unicamp is also gratefully acknowledged.

Author's Contribuitions: Conceptualization, J Labaki and E Mesquita; **Methodology**, J Labaki; **Investigation**, LA Marques and LFV Lima; **Writing - original draft**, LA Marques and LFV Lima; **Writing - review & editing**, J Labaki and E Mesquita**; Funding acquisition**, J Labaki and E Mesquita; **Supervision**, J Labaki and E Mesquita.

Editor: Eduardo Alberto Fancello and Paulo de Tarso Mendonça

References

Bathe, K.J. (2006). *Finite element procedures*. Klaus-Jurgen Bathe.

Bloch, F. (1929). Über die quantenmechanik der elektronen in kristallgittern. Zeitschrift für Physik 52:555-600.

Carneiro, D., Barros, P.L.A., Labaki, J. (2022). Ground vibration attenuation performance of surface walls. Computers and Geotechnics 149.

Doyle, J.F. (1997). Wave propagation in structures: spectral analysis using fast discrete Fourier transforms. Springer (New York).

Elshazly, F.A., Seylabi, E. (2023). On seismic isolation of soil-metafoundation-structure systems. Computers and Geotechnics 161.

Fairweather. G., Karageorghis, A., Martin, P.A. (2003). The method of fundamental solutions for scattering and radiation problems. Engineering Analysis with Boundary Elements 27(7):759–769.

Floquet, G. (1883). Sur les équations différentielles linéaires à coefficients périodiques. Annales Scientifiques de l'École Normale Supérieure 12:47–88.

Jain, S., Pujari, S., Laskar, A. (2021). Investigation of one dimensional multi-layer periodic unit cell for structural base isolation. Structures 34:2151–2163.

Lee, U., Kim, J., Oh, H. (2004). Spectral analysis for the transverse vibration of an axially moving timoshenko beam. Journal of Sound and Vibration 271:685–703.

Nobrega, E.D., Gautier, F., Pelat, A., Dos Santos, J.M.C. (2016). Vibration bandgaps for elastic metamaterial rods using wave finite element method. Mechanical Systems and Signal Processing 79:192–202.

Przemieniecki, J.S. (1968). Theory of Matrix Structural Analysis. McGrall-Hill (New York).

Pu, X., Shi, Z. (2018). Surface-wave attenuation by periodic pile barriers in layered soils. Construction and Building Materials 180:177–187.

Rajapakse, R., Wang, Y. (1991). Elastodynamic Green's functions of orthotropic half plane. Journal of Engineering Mechanics 117(3):588–604.

Rao, S.S. (2011). The Finite Element Method in Engineering (Fifth Edition). Butterworth-Heinemann (Boston).

Shi, Z., Cheng, Z., Xiang, H. (2014). Seismic isolation foundations with effective attenuation zones. Soil Dynamics and Earthquake Engineering 57:143–151.

Xiang, H.J, Shi, Z.F., Wang, S.J., Mo, Y.L. (2012). Periodic materials-based vibration attenuation in layered foundations: experimental validation. Smart Materials and Structures 21.

Xiong, C., Shi, Z., Xiang, H. (2012). Attenuation of Building Vibration Using Periodic Foundations. Advances in Structural Engineering 15:1375–1388.